The chemi-ionization reaction $O+CH \rightarrow HCO^+ + e^-$. Collinear O–CH approach

Aristophanes Metropoulos

Theoretical and Physical Chemistry Institute, National Hellenic Research Foundation, 48 Vass. Constantinou Avenue, Athens 11635, Greece

and

Bernd Engels and Sigrid D. Peyerimhoff

Institut für Physikalische und Theoretische Chemie der Universität Bonn, Wegelerstrasse 12, W-5300 Bonn 1, Germany

Received 26 November 1992; in final form 7 January 1993

We have investigated theoretically the importance of the $O(^3P)+CH(a\,^4\Sigma^-)$ and the $O(^3P)+CH(X\,^2\Pi)$ channels in the collinear chemi-ionization reaction $O+CH \rightarrow HCO^+ + e^-$. We have found that both channels may lead to chemi-ionization via favorable Franck–Condon overlaps with the states of the ionic species.

1. Introduction

Although the generation of HCO^+ in hydrocarbon oxidation has been studied experimentally since 1962 [1], the exact mechanism of its formation, and the electronic or vibronic states involved in the process are still in dispute. The usual assumption is that the ion is generated via the chemi-ionization reaction [2],

$$O(^3P)+CH(X\,^2\Pi) \rightarrow HCO^+(^1\Sigma^+)+e^- . \quad (1)$$

However, there is evidence that low-lying excited states of CH may also be involved in the reaction [2,3]:

$$O(^3P)+CH(a\,^4\Sigma^-) \rightarrow HCO^+(^1\Sigma^+)+e^- , \quad (2)$$

$$O(^3P)+CH(A\,^2\Delta) \rightarrow HCO^+(^1\Sigma^+)+e^- . \quad (3)$$

The somewhat elusive $CH(a\,^4\Sigma^-)$ state has been identified experimentally [4] and is also known from theoretical studies [5]. Along with reaction (1), there is now compelling experimental evidence that reaction (2) is also responsible for the chemi-ionization [6].

To clarify the ionization mechanism for these reactions, an accurate knowledge of the potential surfaces of $HCO^+(^1\Sigma^+)$ and of the ground and excited HCO surfaces is necessary. The ion state has been studied both at the SCF and CI levels but with emphasis on the protonation of CO [7], while states of the neutral radical have been studied at various levels of accuracy but with H+CO as the asymptotic channels [8]. There has been only one theoretical study with reaction (1) in mind, and this has been performed at the INDO level [9]. The most elaborate calculations of the HCO potential surfaces [10], including many electronically excited states, involve only that part of the three-dimensional surface necessary for obtaining the absorption and emission spectrum.

Clearly, a systematic study of the potential energy surfaces of the ground state of HCO^+ and of the ground and low-lying excited states of HCO is necessary for the elucidation of the chemi-ionization mechanism. The primary expectation is that a state of HCO will interact with the continuum of the ground state of HCO^+, thereby losing one electron and forming the ion species. Alternatively, a two-step

process could be considered in which HCO is formed in a particular state and consecutively ionized whereby the energy conservation principle must be considered.

As a first step towards determining an interaction mechanism, we compute those sections of the HCO potential energy surfaces that correspond to the collinear reactions (1) and (2) ($^2\Pi$, $^2\Sigma^+$ and $^2\Delta$ states). The ionic species HCO^+ ($^1\Sigma^+$) is, of course, linear in its equilibrium geometry.

2. Technical details

The calculations have been carried out employing the MRDCI series of programs [11]. The procedure employs a multi-configuration CI with a configuration selection and extrapolation technique which gives a near "singles and doubles" accuracy for the MRD-CI space, using explicitly only a fraction of the original space. In the present calculations we used an accuracy threshold between 3 and 5 μhartree (depending on the region), and this resulted in an average of 25000 configurations for the HCO($^2\Pi$) diagonalization of the HCO Hamiltonian matrix (a maximum of 42 reference configurations considering six electronic states explicitly), an average of 27000 configurations for the HCO($^2\Sigma^+$, $^2\Delta$) states (a maximum of 36 reference configurations considering four electronic states) and an average of 15000 for HCO^+ (25 reference configurations carrying two states).

We have employed the (6-311G**) (s=p exponents for O and C) basis of Krishnan et al. [12] augmented with diffuse p functions on carbon (exponent 0.021) and oxygen (exponent 0.042) to describe the first series of Rydberg states, plus a d function on hydrogen (exponent 1.0) to account for electron correlation (in a balanced treatment with the d functions on the heavier atoms). Eleven electrons were correlated; i.e. the 1s cores of oxygen and carbon were kept doubly occupied in all configurations.

3. Results and discussion

Table 1 shows the correlations between the relevant asymptotic channels of O+CH and the states

Table 1
Correlations between the doublet HCO states and the asymptotic HC+O channels

O	CH	HCO ($C_{\infty v}$)
^3P_g	$X\,^2\Pi$	$^2\Sigma^-$, $^2\Sigma^+$, $^2\Pi$, $^2\Delta$
^3P_g	$a\,^4\Sigma^-$	$^2\Sigma^+$, $^2\Pi$
^1D_g	$X\,^2\Pi$	$^2\Sigma^-$, $^2\Sigma^+$, (2)$^2\Pi$, $^2\Delta$, $^2\Phi$

of the resulting HCO. The quartet and sextet states are not considered in the present work. Both the $O(^3P)+CH(X\,^2\Pi)$ and the $O(^3P)+CH(a\,^4\Sigma^-)$ channels correlate with the two lowest $^2\Pi$, and the two lowest $^2\Sigma^+$ states of HCO, while the first $^2\Delta$ state of HCO correlates with the first channel above. The third and fourth $^2\Pi$ states correlate with the $O(^1D)+CH(X\,^2\Pi)$ channel.

We have calculated at the CI level the first four $^2\Pi$, the first three $^2\Sigma^+$, and the first $^2\Delta$ states of HCO and the ground $^1\Sigma^+$ state of HCO^+. The calculated states are shown in tables 2 and 3, and depicted in figs. 1 and 2. The lowest $^2\Pi$ state possesses in the linear geometry the electronic configuration KK $3\sigma^2 4\sigma^2 5\sigma^2 1\pi^4 2\pi$ (shorthand notation $\sigma^2\pi^4\pi^*$) and must be considered a pure valence state. It is well known that this state exhibits a Renner–Teller effect, i.e. splits into two components upon bending, whereby the lower component prefers the bent geometry ($X\,^2A'$, ... $5a'^2 6a'^2 1a''^2 7a'$) around 120°, and the upper component remains linear. The barrier towards linearity is around 1.15 eV [10].

At small O–CH separations the first excited $^2\Pi$ states possess Rydberg character and for this reason exhibit potential minima at the same geometry as the ionic HCO^+ state (fig. 1) being the limit of the Rydberg series. The position of the $2\,^2\Pi$ ($\pi^* \rightarrow 3p\pi$) should be calculated reliably, the higher Rydberg states would require optimal $4p\pi$ and $3d\pi$ functions not explicitly included in the present calculation. More details can be found in ref. [10].

At larger O–CH separations there are avoided crossings with repulsive valence-type states (fig. 1). The potential curve for the collinear $O(^3P)+CH(X\,^2\Pi)$ approach is found to be repulsive enough to make reactions at thermal energies unlikely. On the other hand, the second channel $O(^3P)+CH(a\,^4\Sigma^-)$ is found to be attractive, and due to the intersystem crossing with the lowest $^2\Pi$

Table 2
Selected values of the HCO($^2\Pi$) and HCO^+($^1\Sigma^+$) potential energy curves. All quantities in au

R	HCO(X $^2\Pi$)	HCO(2 $^2\Pi$)	HCO(3 $^2\Pi$)	HCO(4 $^2\Pi$)	HCO^+(X $^1\Sigma^+$)
1.6	−113.0898	−113.0321	-	-	−112.9672
1.7	−113.2659	−113.2039	−113.1340	-	−113.1236
1.8	−113.3869	−113.3074	−113.2336	-	−113.2238
1.9	−113.4666	−113.3675	−113.2901	−113.0760	−113.2828
2.0	−113.5155	−113.3979	−113.3189	−113.1667	−113.3123
2.1	−113.5442	−113.4047	−113.3255	−113.2317	−113.3207
2.2	−113.5568	−113.3977	−113.3187	−113.2776	−113.3143
2.3	−113.5578	−113.3806	−113.3118	−113.2989	−113.2983
2.4	−113.5514	−113.3592	−113.3297	−113.2933	−113.2754
2.5	−113.5388	−113.3444	−113.3313	−113.3047	−113.2484
2.6	−113.5232	−113.3477	−113.3104	−113.3049	−113.2200
2.7	−113.5060	−113.3484	−113.3109	−113.2764	-
2.8	−113.4884	−113.3472	−113.3103	−113.2758	−113.1575
2.9	−113.4695	−113.3416	−113.3062	−113.2714	-
3.0	−113.4520	−113.3367	−113.3029	−113.2682	−113.0989
3.1	−113.4336	−113.3298	−113.2957	−113.2618	-
3.2	−113.4165	−113.3205	−113.2876	−113.2560	−113.0513
3.3	−113.3993	−113.3129	−113.2790	−113.2479	-
3.4	−113.3852	−113.3043	−113.2723	−113.2416	−113.0115
3.5	−113.3725	−113.2960	−113.2652	−113.2405	−112.9939
3.6	−113.3617	−113.2894	−113.2572	−113.2392	−112.9808
3.7	−113.3514	−113.2820	−113.2497	−113.2471	-
3.8	−113.3426	−113.2746	−113.2526	−113.2452	−112.9590
3.9	−113.3341	−113.2686	−113.2608	−113.2385	-
4.0	−113.3276	−113.2690	−113.2641	−113.2330	−112.9388
4.1	−113.3227	−113.2745	−113.2622	−113.2272	-
4.2	−113.3182	−113.2803	−113.2577	−113.2242	−112.9238
4.3	−113.3146	−113.2856	−113.2538	−113.2216	-
4.4	−113.3120	−113.2898	−113.2509	−113.2195	−112.9123
4.5	−113.3095	−113.2932	−113.2456	−113.2180	-
4.6	−113.3079	−113.2968	−113.2448	−113.2187	−112.9060
4.7	−113.3064	−113.3000	−113.2432	−113.2216	-
4.8	−113.3052	−113.3025	−113.2420	−113.2239	−112.9016
4.9	−113.3050	−113.3046	−113.2422	−113.2264	-
5.0	−113.3075	−113.3041	−113.2423	−113.2290	−112.9007
5.3	−113.3112	−113.3035	−113.2411	−113.2330	-
5.7	−113.3156	−113.3013	−113.2410	−113.2367	-
6.0	−113.3162	−113.3011	−113.2408	−113.2377	−112.8926
8.0	−113.3190	−113.3009	−113.2404	−113.2394	−112.8880
10.0	−113.3189	−113.3006	−113.2405	−113.2395	−112.8899
20.0	−113.3191	−113.3008	−113.2406	−113.2397	−112.8915

state around 5 bohr, there is a certain probability of a transition from the second channel to the X $^2\Pi$ state. The HCO^+ minimum lies in the region of high-lying vibrational levels of the X $^2\Pi$ state, and a favorable Franck–Condon overlap may generate the ionic species.

The calculated energy differences between the asymptotic channels are 0.5 and 2.14 eV (table 2) instead of the experimentally known differences 0.72 eV (X $^2\Pi$–a $^4\Sigma^-$ of CH) and 1.97 eV (O(^{3}P)–O(^{1}D)). There are also slight discrepancies in the calculated energies for the same asymptotic channels resulting from different spatial wavefunctions (−113.3006 hartree for 2 $^2\Pi$, −113.3010 hartree for 2 $^2\Sigma^+$, −113.3189 hartree for X $^2\Pi$ and −113.3173 hartree for 1 $^2\Sigma^+$) which amount to less than 0.05

Table 3
Selected values of the HCO $^2\Sigma^+$ and $^2\Delta$ potential energy curves. All quantities in au

R	HCO($1\,^2\Sigma$)	HCO($2\,^2\Sigma$)	HCO($3\,^2\Sigma$)	HCO($1\,^2\Delta$)
1.6	−113.0993	−113.0903	−113.0222	-
1.7	−113.2561	−113.2489	−113.1799	-
1.8	−113.3587	−113.3507	−113.2812	-
1.9	−113.4157	−113.4113	−113.3392	-
2.0	−113.4470	−113.4415	−113.3672	-
2.1	−113.4609	−113.4488	−113.3751	-
2.2	−113.4581	−113.4408	−113.3697	-
2.3	−113.4470	−113.4253	−113.3548	-
2.4	−113.4312	−113.4038	−113.3334	-
2.5	−113.4166	−113.3768	−113.3131	-
2.6	−113.4015	−113.3536	−113.2881	-
2.8	−113.3765	−113.2974	−113.2369	−113.2108
3.0	−113.3591	−113.2389	-	−113.2316
3.2	−113.3489	−113.2506	-	−113.2495
3.4	−113.3381	−113.2602	-	−113.2647
3.6	−113.3305	−113.2683	-	−113.2768
3.8	−113.3252	−113.2751	-	−113.2868
4.0	−113.3230	−113.2801	-	−113.2953
4.2	−113.3193	−113.2859	-	−113.3014
4.4	−113.3152	−113.2926	-	−113.3061
4.6	−113.3161	−113.2960	-	−113.3102
4.8	−113.3169	−113.2966	-	−113.3130
5.0	−113.3173	−113.2982	-	−113.3147
5.2	−113.3170	−113.2997	-	−113.3153
5.4	−113.3168	−113.3000	-	−113.3156
5.6	−113.3169	−113.3005	-	−113.3160
5.8	−113.3168	−113.3006	-	−113.3161
6.0	−113.3169	−113.3006	-	−113.3169
7.0	−113.3170	−113.3007	-	−113.3170
10.0	−113.3173	−113.3010	-	−113.3169

eV. This is an indication that there is a small imbalance in the description of the states, but this is acceptable here since our purpose is not to generate the most accurate O–CH curves but to assess the involvement of the excited states in the chemi-ionization reaction that generates HCO^+.

Fig. 2 shows three $^2\Sigma^+$ and one $^2\Delta$ HCO states. The lowest $^2\Sigma^+$ can be characterized as a valence state, the next two as Rydberg 3s and Rydberg 3pσ states exhibiting again the same characteristics as the ionic HCO^+ species. The minimum of the 3s state is considerably below that of the $2\,^2\Pi$ (3pπ) state (tables 2, 3); the $^2\Sigma^+$ (3pσ) minimum is higher than the related $2\,^2\Pi$ (3pπ) minimum as found elsewhere [10]. Again, at larger O–CH separations interactions occur with repulsive valence-type states. Since there are no Rydberg d functions in the AO basis, the curve of the $^2\Delta$ state has not been followed to small O–CH separations. Likewise, the interaction of $3\,^2\Sigma^+$ with higher states in the dissociation channels has not been investigated further.

It is evident that both the $^2\Sigma^+$ HCO state arising from the $O(^3P)+CH(a\,^4\Sigma^-)$ channel and the $^2\Delta$ state arising from the lower $O(^3P)+CH(X\,^2\Pi)$ channel are repulsive and they cannot lead to chemi-ionization. On the other hand, the lowest $^2\Sigma^+$ state, also arising from the lower $O(^3P)+CH(X\,^2\Pi)$ channel, is attractive in the collinear O+CH approach. Its potential minimum is at the linear arrangement of the nuclei, but it shows heavy mixing with the $2\,^2\Sigma^+$ (3s) state upon bending [10] and at smaller O–CH separations as is obvious from fig. 2. Again, the HCO^+ minimum lies in the region of high-lying vibrational levels of this $1\,^2\Sigma^+$ state, and a fa-

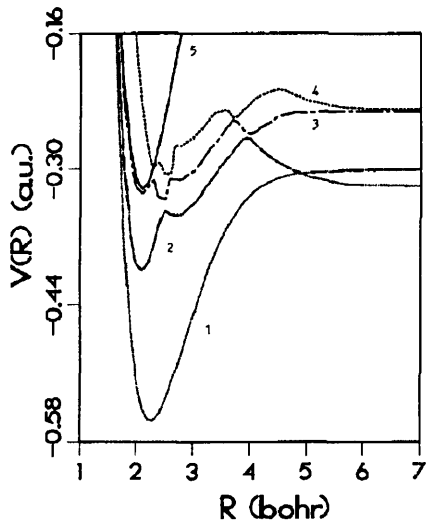

Fig. 1. The four lowest $^2\Pi$ states of HCO (1 through 4), and the ground $^1\Sigma^+$ state of HCO^+ (5) as a function of O–CH separation (all relative to −113.0000 au). Asymptotic HCO channels: 1: $O(^3P)+CH(X\,^2\Pi)$; 2: $O(^3P)+CH(a\,^4\Sigma^-)$; 3: $O(^1D)+CH(X\,^2\Pi)$; 4: $O(^1D)+CH(X\,^2\Pi)$.

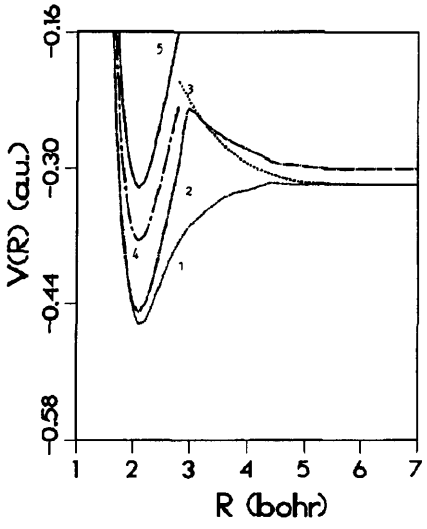

Fig. 2. The two lowest $^2\Sigma^+$ (1, 2), the first $^2\Delta$ (3), and the Rydberg $^2\Sigma^+$ (4) states of HCO, and the ground $^1\Sigma^+$ state of HCO^+ (5) as a function of O–CH separation (all relative to −113.0000 au). Asymptotic HCO channels: 1: $O(^3P)+CH(X\,^2\Pi)$; 2: $O(^3P)+CH(X\,^2\Pi)$; 3: $O(^3P)+CH(a\,^4\Sigma^-)$.

vorable Franck–Condon overlap may lead to chemi-ionization.

In conclusion, HCO^+ may be formed either by the $O(^3P)+CH(X\,^2\Pi)$ channel via the $HCO(1\,^2\Sigma^+)$ state or by the $O(^3P)+CH(a\,^4\Sigma^-)$ channel via the $HCO(X\,^2\Pi)$ state, provided that the non-adiabatic transition probability between the second channel and the $X\,^2\Pi$ state at their avoided crossing is reasonably large. In both cases a favorable Franck–Condon overlap between the high-lying vibrational states of the neutral and low-lying vibrational states of the ionic species is essential for the formation of the ion. Further investigation of this system, including bent geometries, is under way.

Acknowledgement

We thank Professor Kyle D. Bayes for bringing this system to our attention and for his valuable suggestions. One of us (AM) thanks the Deutsche Forschungsgemeinschaft (SFB 334) for supporting him while at the Universität Bonn. Part of this work was done at the Computer Center of the University of Bonn and part on the FPS-500 computer of the National Hellenic Research Foundation in Athens.

References

[1] H.F. Calcot, 8th International Symposium on Combustion (Williams and Williams, London, 1962) p. 184.
[2] K.D. Bayes, Chem. Phys. Letters 152 (1988) 424.
[3] D.E. Phippen and K.D. Bayes, Chem. Phys. Letters 164 (1989) 625.
[4] T. Nelis, J.M. Brown and K.M. Evenson, J. Chem. Phys. 88 (1988) 2087; 92 (1990) 4067;
A. Kasdan, E. Herbst and W.C. Lineberger, Chem. Phys. Letters 31 (1975) 78.
[5] G.C. Lie, J. Hinze and B. Liu, Chem. Phys. 59 (1973) 1887; 59 (1973) 1872; 57 (1972) 625;
H.P.D. Liu and G. Verhaegen, J. Chem. Phys. 53 (1970) 735.
[6] Z. Hou and K.D. Bayes, J. Phys. Chem. 96 (1992) 5685.
[7] D. Talbi, A.P. Hickman, F. Pauzat, Y. Ellinger and G. Berthier, Astrophys. J. 339 (1989) 231;
D. Talbi, F. Pauzat and Y. Ellinger, Chem. Phys. 126 (1988) 291;
D. Talbi and F. Pauzat, Astron. Astrophys. 181 (1987) 394;
P.J. Bruna, S.D. Peyerimhoff and R.J. Buenker, Chem. Phys. 10 (1975) 323.
[8] T.H. Dunning Jr., J. Chem. Phys. 73 (1980) 2304;
K. Tanaka and E.R. Davidson, J. Chem. Phys. 70 (1979) 2904;

P.J. Bruna, R.J. Buenker and S.D. Peyerimhoff, J. Mol. Struct. 32 (1976) 217;
G.F. Adams, G.D. Bent, G.D. Purvis and R.J. Bartkett, J. Chem. Phys. 71 (1971) 3697.
[9] M. MacGregor and R.S. Berry, J. Phys. B 6 (1973) 181.
[10] H. Lorenzen-Schmidt, M. Peric and S.D. Peyerimhoff, Chem. Phys. submitted for publication.
[11] R.J. Buenker and S.D. Peyerimhoff, Theoret. Chim. Acta 35 (1974) 33; 39 (1975) 217; in: New Horizons of Quantum Chemistry, eds. P.O. Lowdin and B. Pullmann (Reidel, Dordrecht, 1983) pp. 183–219.
[12] R. Krishnan, J.S. Binkley, R. Seeger and J.A. Pople, J. Chem. Phys. 72 (1980) 650.